Measurements of Resonant Electron Capture in He^+ on He Collisions*

GRANT J. LOCKWOOD,† HERBERT F. HELBIG, AND EDGAR EVERHART
Physics Department, University of Connecticut, Storrs, Connecticut
(Received 1 July 1963)

Differential scattering of He^+ ions by He atoms in the energy range of 0.4 to 25.0 keV has been studied as a function of scattering angle between 0.4 and 4.4°. The scattered ion was analyzed to determine whether it had captured an electron after a single collision with a target atom. The limits in both energy and angle were chosen in order that a very wide variation in velocity and in impact parameter might be represented by the data. The high angular resolution needed in obtaining data at the small angles placed severe requirements on the beam-defining geometry and made precise determinations of the ion beam direction necessary. In addition, a spreading of the low-energy ion beam, which would have prevented taking data at small angles, was observed. The use of a special high-temperature collision chamber was necessary to prevent this spreading. Besides electron-capture effects, electron stripping and double capture were also studied, as represented by the He^{++} and He^- components among the scattered particles. For this ion-atom combination, electron capture by the ion is a result of resonant charge transfer and the electron capture probability is observed to oscillate when plotted versus incident ion energy. However, the electron-capture probability, which is found to be independent of scattering angle at the high ion energies, is observed to undergo a transition such that the electron-capture probability oscillates rapidly with angle, and is independent of ion energy at low energies. From these data, relationships among electron-capture probability, scattering angle, and ion energy are found and used to obtain an empirical equation that fits the data. This paper is the first of two consecutive papers, of which the second, by Everhart, analyzes these data in terms of the theory of resonant electron capture.

1. INTRODUCTION

RESONANT electron capture in violent atomic collisions was first observed by Ziemba and Everhart,[1] who studied the combination He^+ on He. The electron-capture probability P_0, for a fixed 5° scattering angle, showed a resonant structure with seven peaks when plotted against incident ion energy in the range from 1 to 200 keV. Resonant structure has been found in other ion-atom combinations.[2–4] These earlier studies were confined to a determination of the dependence of P_0 on either the velocity of collision[1–3] or on the impact parameter.[2,4] Notably, the previous He^+ on He work studied only violent collisions wherein the impact parameter was nearly zero on an atomic scale over the entire energy range studied.

The present study of He^+ on He was conducted to determine the dependence of P_0 on both velocity and impact parameter over a very wide range in both, with particular interest in the very gentle collisions, i.e., those in which the particle is scattered only a fraction of a degree at low energies. To accomplish this, the experimental apparatus was designed for measuring differential scattering from 0.4 to 4.4° in the energy range from 0.43 to 25 keV. The percentages of He^{++} and He^- in the scattered beam were also determined, but this was done at 1.5° only.

Section 2 describes the apparatus and procedure with particular attention to those features which were necessary to allow differential measurements to be made for particles scattered at very small angles from the direction of the incident beam. The data are presented and discussed in Sec. 3, where the dependences of P_0 on incident energy and scattering angle are shown. Section 4 presents and discusses empirical relationships which fit the data.

An analysis of the present data in terms of the existing theory for resonant charge transfer is given in a second paper[5] immediately following in this journal.

The differential data obtained here at 1 keV are analyzed further elsewhere in a brief paper[6] to show their relationship to the total cross section for charge transfer at that energy.

2. APPARATUS AND PROCEDURE

The University of Connecticut 200-kV Cockcroft-Walton accelerator was used in this work. This machine and the associated apparatus have been used in several similar investigations[1–3] of other ion-atom combinations. The description below is brief except where it concerns improvements and new features arising in the present study.

* This work was supported by the U. S. Army Research Office, Durham, North Carolina, and the U. S. Air Force Cambridge Research Laboratories.

† Present address: Sandia Corporation, Albuquerque, New Mexico.

[1] F. P. Ziemba and E. Everhart, Phys. Rev. Letters **2**, 299 (1959).

[2] F. P. Ziemba, G. J. Lockwood, G. H. Morgan, and E. Everhart, Phys. Rev. **118**, 1552 (1960).

[3] G. J. Lockwood and E. Everhart, Phys. Rev. **125**, 567 (1962).

[4] P. R. Jones, P. Costigan, and G. Van Dyk, Phys. Rev. **129**, 211 (1963).

[5] E. Everhart, Phys. Rev. following paper, **132**, 2083 (1963).

[6] E. Everhart, H. F. Helbig, and G. J. Lockwood, in Proceedings of the Third International Conference on the Physics of Electronic and Atomic Collisions (to be published).

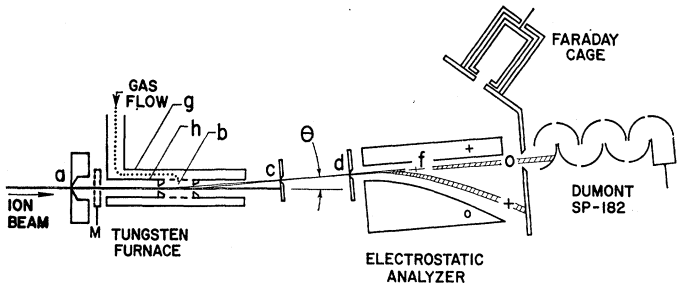

FIG. 1. The collision chamber and the associated detection apparatus.

a. The Scattering Apparatus

The collision chamber and associated detection apparatus are shown in Fig. 1. The incident ion beam enters the collision chamber (tungsten furnace) through hole a, which is part of a two-hole collimating system. Immediately inside hole a is a Faraday cup monitor M which can be moved into the path of the beam to measure its intensity, or moved aside to allow the beam to pass through the collision chamber. In the vicinity of b the incident beam encounters the target helium gas, and a small fraction of the incident ions are scattered to the chosen angle θ defined by apertures c and d, which follow the collision chamber. Only those particles scattered through this angle can reach the detector. Following c and d is an electrostatic analyzer by which either the total scattered beam (as defined by c and d) or its neutral component is admitted to the detector. The number of neutral particles divided by the total number of scattered particles is the electron capture probability P_0. The properties of the detecting system and the count procedures are fully discussed in the paper by Ziemba *et al.*[2]

b. Need for High Temperature

The furnace-type collision chamber used in this experiment is the same chamber that was used to produce atomic hydrogen for the H^+ on H study.[3] The elaborate construction and the ability to heat the chamber to 2400°K were necessary to make atomic hydrogen in that earlier experiment. This type of chamber was also found to be necessary in this present experiment. Heating provided a quick and efficient way of outgassing the collision chamber, thus reducing the correction for residual gas. This was most important at the small angles where it was found necessary to keep the target gas pressure low to assure single-collision conditions.

Although a lower temperature would have been sufficient for outgassing, high temperature was needed for another reason. It was found, when working at low energies, that the incident He^+ beam spread symmetrically while in the region of the collision chamber. In this region the beam passes close to many surfaces and finally strikes the end of the chamber. It was concluded that this spreading was caused by scattered particles charging nonconducting layers on these surfaces. Fortunately this effect could be eliminated by heating the chamber to 2000°K. The spreading of the ion beam would otherwise have interfered with the small-angle scattered beams and completely prevented taking small-angle data. Although the exact mechanism for eliminating this effect is unknown, a plausible explanation is that when the furnace is heated to 2000°K the region has sufficient electrons to neutralize any charged surfaces.

c. Beam Collimation

The apertures used to collimate the incident ion beam and the holes c and d which define the scattered beam were made very small in this study in order to increase the resolution. At the same time, this made it geometrically possible to take differential measurements at very small angles. Hole a and the hole (not shown) preceding it were 0.382 mm in diam, c was a slit 3.18 mm long and 0.0728 mm wide with the long axis perpendicular to the plane containing the scattering angle, and d was a hole 0.126 mm in diam. The small size of the apertures c and d and their location at 33.1 and 60.6 mm, respectively, from the scattering center b, produced an angular resolution of $\pm 0.18°$ and allowed useful measurements to be made at angles as small as 0.4° from the direction of the incident beam.

d. Scattering Angle Determination

Because data were to be taken within 0.4° of the main beam, ordinary mechanical determination of incident beam direction was inadequate and the following procedure was used. That part of the apparatus containing the collimating apertures c and d, the electrostatic analyzer, and the detecting system, can be rotated about the scattering center b through an angular range from $+4.4$ to $-4.2°$. This motion about b allows the scattering angle θ to be varied and a vernier on the angular scale permits reproducible settings to the closest 0.1°. The true zero, from which all other angles are measured, is determined from the symmetry of the plot of the scattered current versus scale angle in both the positive and negative angle regions. This true zero determination was repeated at each energy where measurements were made. The

maximum variation of incident beam direction was found to be less than 0.1°.

e. The Electrostatic Analyzer

The electrostatic analyzer which follows the scattered beam defining apertures c and d, served two functions in this experiment. First, it was used to charge-analyze the scattered beam. Thus, with both the flat and curved plates grounded, the total scattered beam, comprised of both charged and neutral particles, enters the detector when it is in the position shown in Fig. 1. If then, with the detector held fixed, a sufficient positive voltage is applied to the flat plate, all charged particles are swept away and the neutral component alone is detected. The detector is then rotated about f to a position indicated by the + beam in Fig. 1. With the detector in this position the voltage on the flat plate can be increased from zero until the He^{++} component alone is swept into the detector. Further increase of the voltage on the flat plate will sweep the He^{++} component past the detector and allow the He^{+} component to be detected. Under these conditions, if the magnitude of the voltage is held fixed but its polarity reversed, the He^{-} component can be detected.

The second use of the electrostatic analyzer was to determine the energy of the ion beam at low energies. This energy was found to be 70±50 eV higher than the power supply voltage would indicate. The difference arises because the plasma in the glass rf source bottle is not at the exact potential of the metal source exit canal. Variations in the plasma potential occur when the source parameters are changed. To use the analyzer for determining the ion beam energy it is necessary to know the analyzer voltage which would deflect the ion beam a fixed distance. Plotting detected current versus analyzer voltage, a broad flat profile is obtained as the scattered beam is swept across the entrance to the detector. However, the half-maximum value of current on the sharply rising leading edge of this profile provides an accurate voltage reference point V, which is proportional to the beam energy T, according to the equation $T=kV$. The calibration constant k is, of course, the same at any voltage. This calibration was carried out at 30 keV where the source plasma's contribution was less than 0.3% of the total ion energy.

3. DATA AND DISCUSSION

The data presented here show the dependence of electron capture probability P_0 on the two experimental variables, incident ion energy T and laboratory scattering angle θ.

Figure 2 plots P_0 versus T for scattering angles fixed at 5, 3, and 1°. The 5° data, taken from the paper by Ziemba *et al.*[2] show that P_0 oscillates as a function of energy over the entire energy range plotted. The present 3° data show a similar oscillation, which starts in phase with the 5° data at high energies, but goes out of

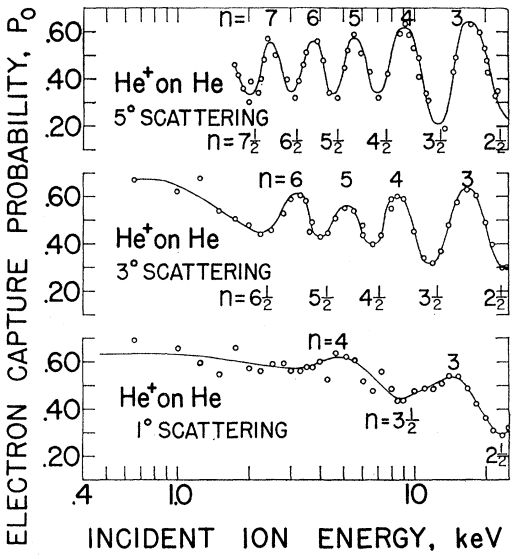

FIG. 2. The electron-capture probability P_0 is plotted versus incident ion energy T in keV for the combination He^+ on He. These data are for scattering angles of 5, 3, and 1°; laboratory coordinates. The graphs show how the oscillation in P_0 changes with scattering angle. The maxima and minima are identified by indices n.

phase at lower energies and finally stops oscillation altogether, below about 2 keV. The 1° data exhibit the same trend with even more of a phase shift and with oscillation ceasing at an even higher energy.

The 5° studies of this He^+ on He collision have shown that a peak in P_0 at about 250 keV is the first, $n=1$, in the series, with successive peaks at 43, 17.5 keV, etc. Consistent with these results, the peaks of Fig. 2 are labeled with indices $n=3$ to $n=8$, with the valleys being assigned half-integral values.

Figure 3 shows the variation in P_0 as a function of θ for fixed energies of 25, 8, 5, and 1 keV. These four are shown here because they represent how P_0 varies with θ in the three energy regions of interest, namely at 25 keV where P_0 is independent of angle for all but the smallest angles, at 8 and 5 keV where P_0 is in the transition region from energy dependence to angular dependence and finally at 1 keV where P_0 is independent of energy for all angles measured and oscillates rapidly as a function of angle.

The transition of P_0 from energy dependence to angular dependence, and an over-all view of the phenomena can best be seen on Fig. 4. Here the location of the several maxima and minima are shown on T versus θ coordinates. Each solid curve shows the position of a particular peak or valley and these are numbered with the n values discussed above.

A qualitative comparison of these data with those obtained for other ion-atom collisions shows these energy-dependent oscillations to be similar to those found for the fixed-angle studies of He^+ on He, H^+ on He, and H^+ on H_2 by Ziemba *et al.*,[2] and those of H^+

on H and H^+ on H_2 by Lockwood and Everhart.[3] A figure similar to Fig. 4, showing both the angular and the energy dependence of P_0, has been given by Jones *et al.*[4] for the Ne^+ on Ne system.

Most of the previous experiments above have been interpreted within a theoretical framework similar to that of Bates, Massey, and Stewart,[7] and the following paper[5] in this journal will analyze the present data in this same framework including, where possible, the latest modifications to the theory. These new data at low energies and small scattering angles offer an opportunity to learn details of the He^+ on He interaction at moderately large internuclear distances.

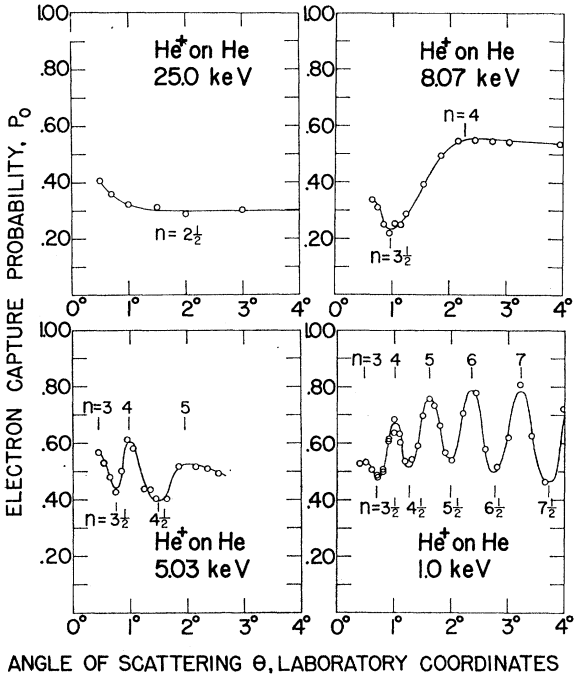

FIG. 3. The electron-capture probability P_0 is plotted versus laboratory scattering angle θ for the combination He^+ on He. These data are for incident ion energies of 25, 8.07, 5.03, and 1.0 keV. The maxima and minima are identified by the indices n.

The probability of electron stripping P_2, as determined by the He^{++} production in these collisions, was also measured here in the energy range of 3 to 25 keV at a fixed scattering angle of 1.5°. These data, as shown in Fig. 5(a), have no simple phase relationship to the P_0 oscillations at this same angle. The data are scanty, but there is a possibility that P_2 exhibits a resonant-like phenomenon which is relatively independent of the P_0 resonances in phase and peak location.

A trace of a He^- component was seen among the scattered particles at 1.5°, and this P_{-1} fraction, as plotted in Fig. 5(b), did not exceed 0.23%.

[7] D. R. Bates, H. S. W. Massey, and A. L. Stewart, Proc. Roy. Soc. (London) A216, 437 (1953). See also O. B. Firsov, Zh. Eksperim. i Teor. Fiz. 21, 1001 (1951), and T. Holstein, J. Phys. Chem. 56, 832 (1952)

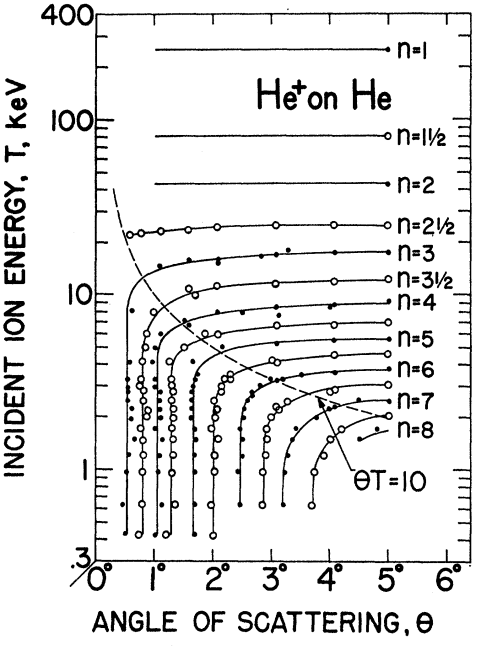

FIG. 4. The locations of the maxima and minima in the electron-capture probability P_0 are displayed on T versus θ axes, where the incident ion energy T is in keV and the laboratory scattering angle θ is in degrees. The maxima and minima are identified by the indices n.

4. EMPIRICAL RELATIONSHIPS

When P_0 is plotted versus reciprocal velocity or $T^{-1/2}$, in the region on Fig. 4 where P_0 is substantially independent of θ, it is seen that the spacings between adjacent maxima are approximately equal. Such plots are seen in Fig. 1 of Ref. 1 and Fig. 3 of Ref. 2 and are consistent with a linear dependence of n on $T^{-1/2}$. If the high-energy data of Ziemba *et al.*[2] are included with the present data, the expression

$$n-\tfrac{1}{4}=11.4T^{-1/2}, \qquad (1)$$

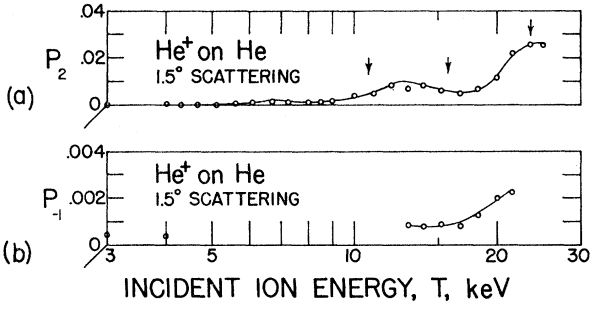

FIG. 5. (a) The probability of electron stripping P_2 is plotted versus incident ion energy T in keV for the combination He^+ on He. These data are for the scattering angle of 1.5° laboratory coordinates. The arrows indicate the locations of a valley, a peak, and a valley, respectively, in the P_0 data at this same angle. (b) The probability of double electron capture P_{-1} is plotted versus incident ion energy T in keV for the He^+ on He combination. These data are for the scattering angle of 1.5° laboratory coordinates.

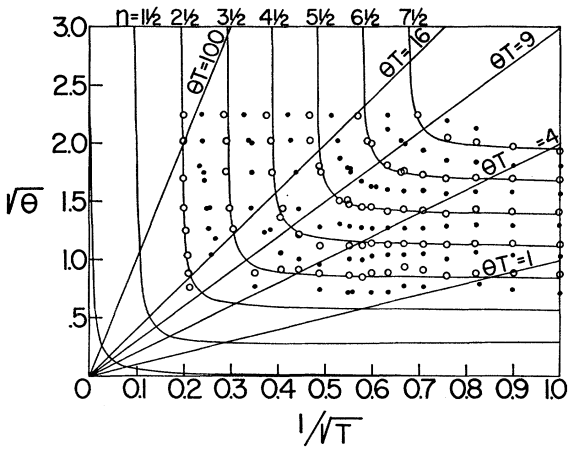

FIG. 6. The locations of the maxima and minima in the electron-capture probability P_0 are displayed on $\theta^{1/2}$ versus $T^{-1/2}$ axes, where the laboratory scattering angle θ is in degrees and the incident ion energy T is in keV. The solid lines which are seen to fit the data are given by empirical equation (see Eq. 6). The maxima and minima are identified by the indices n.

with T in keV, describes the data fairly well between $n=1$ and $n=6$. However, if only the present data are used, the expression

$$n-\tfrac{1}{2}=10.5T^{-1/2} \tag{2}$$

fits the data somewhat better between $n=3$ and $n=8$.

These equations are supported approximately but not exactly by the theory. The following paper[5] shows that the multiplier of $T^{-1/2}$ or $1/v$, varies somewhat depending on the impact parameter even for data taken at a constant angle, and that the term which is approximated by $\frac{1}{4}$ or $\frac{1}{2}$ in Eqs. (1) and (2) also varies slowly. Nonetheless, the above expressions fit the data moderately well within the ranges specified.

A more satisfactory situation obtains at low energies where P_0 and n are seen in Fig. 4 to be functions of θ, but not energy. Here it is found empirically that the index n varies as $\theta^{1/2}$, and that the equation

$$n-\tfrac{1}{2}=3.5\theta^{1/2}, \tag{3}$$

with θ in degrees, fits the data well. A simple dimensional argument can be used with the theory to support the form of Eq. (3) exactly: Starting with Eq. (5) of the paper which follows,[5] and dropping a phase term which is negligible at low velocities, the result is

$$n-\tfrac{1}{2}=J/(hv), \tag{4}$$

where h is Planck's constant, v is the velocity, and J is a factor which depends only on the impact parameter. However, Eq. (11) of the same paper[5] shows that, quite generally, the impact parameter depends only on the product θT. Using these results, and replacing v by $T^{1/2}$, Eq. (4) may be written as

$$n-\tfrac{1}{2}=bJ(\theta T)/T^{1/2}=b\theta^{1/2}[J(\theta T)/(\theta T)^{1/2}], \tag{5}$$

where b absorbs the various constants. The bracketed term is a function only of the product θT. The experimental fact that the data of this region do not depend on T but do depend on θ requires that the bracketed term must be a constant independent of θT, i.e., $J(\theta T)$ must here be proportional to $(\theta T)^{1/2}$. Thus, Eq. (3) is supported theoretically, and the numerical value of the constant in that equation gives a useful measure of a quantity J which enters the theory. It must be noted, however, that the $\theta^{1/2}$ dependence of Eqs. (3) and (5) can apply specifically only in regions where the data are found experimentally to be independent of T.

In considering the transition region, the asymptotic dependence on $T^{-1/2}$ and $\theta^{1/2}$ suggested a plot of all the data as on Fig. 6 where lines of constant n are shown on $T^{-1/2}$ versus $\theta^{1/2}$ coordinates. Here the data points fit fairly well a family of hyperbolas, shown by the solid lines, whose equation is

$$[\theta^{1/2}-(n-\tfrac{1}{2})/3.5][T^{-1/2}-(n-\tfrac{1}{2})/10.5]=6.6\times10^{-3} \tag{6}$$

with θ in degrees and T in keV.

It will be seen[5] that the analysis only approximately describes the data of Fig. 4. In its present form it would not predict Eq. (6). However, this empirical equation is a moderately accurate, simple, and useful description of all the experimental data.